

The Effects of Long-Term Spinal Cord Injury on Mechanical Properties of the Rat Urinary Bladder

KEVIN K. TOOSI,^{1,2} JIRO NAGATOMI,^{1,2} MICHAEL B. CHANCELLOR,³ and MICHAEL S. SACKS^{1,2}

¹Engineered Tissue Mechanics and Mechanobiology Laboratory, Department of Bioengineering, University of Pittsburgh, Pittsburgh, PA 15219, USA; ²McGowan Institute for Regenerative Medicine, University of Pittsburgh, 100 Technology Drive, Room 234, Pittsburgh, PA 15219, USA; and ³Department of Urology, University of Pittsburgh, Pittsburgh, PA 15219, USA

(Received 5 August 2007; accepted 16 June 2008; published online 12 July 2008)

Abstract—We have demonstrated that bladder wall tissue in spinal cord injury (SCI) rats at 10 days post-injury is more compliant and accompanied by changes in material class from orthotropic to isotropic as compared to normal tissue. The present study examined the long-term effects (3-, 6-, and 10-weeks) post-SCI on the mechanical properties of bladder wall tissues, along with quantitative changes in smooth muscle orientation and collagen and elastin content. Bladder wall compliance (defined as $\det(\mathbf{F}) - 1$ under an equi-biaxial stress state of 100 kPa, where \mathbf{F} is the deformation gradient tensor) was found to be significantly greater at 3- and 6-weeks (0.873 ± 0.092 and 0.864 ± 0.112 , respectively) when compared to the normal bladders (0.260 ± 0.028), but at 10 weeks the compliance reduced (0.389 ± 0.061) to near that of normal bladders. This trend in mechanical compliance closely paralleled the collagen/elastin ratio. Moreover, changes in material class, assessed using a graphical technique, correlated closely with quantitative changes in smooth muscle fiber orientation. The results of the present study provide the first evidence that, while similarities exist between acute and chronic responses of the urinary bladder wall tissue to SCI, the overall alterations are distinct, result in profound and complex time dependent changes in bladder wall structure, and will lay the basis for simulations of the bladder wall disease process.

Keywords—Bladder wall, Spinal cord injury, Biomechanics, Remodeling.

INTRODUCTION

Approximately 250,000–400,000 individuals in the United States have spinal cord injuries (SCIs), with urologic complications among the most common clinical conditions.³ Specifically, spinal cord injuries rostral to the lumbar spine can cause severe lower urinary tract dysfunctions including overactive bladders and urinary

retention.⁶ These bladder abnormalities are reportedly accompanied not only by changes in the bladder wall tissue morphology, including increased thickness,¹⁷ fibrosis⁵ and trabeculation,²¹ but also by drastic changes in the mechanical properties of the wall.^{10,24,30} Although extensive studies have been conducted on the effects of SCI on bladder function,^{3,6,15,19,29,31} the alterations in mechanical behavior and functional properties of the bladder wall tissue and the underlying mechanisms are not well understood.

Previously our laboratory has demonstrated that the bladder wall tissue in a rat model of SCI was significantly more compliant 10 days post-SCI compared to the normal rat bladder. Furthermore, 10-day SCI rat bladder changed its material class following SCI; behaving as an isotropic material while normal rat bladder was mechanically anisotropic.⁹ In addition to the changes in compliance and material class, biochemical assays revealed that while collagen concentration decreased, the elastin concentration of 3-week SCI bladders was significantly greater than normal bladders.¹⁸ Finally, using a novel image analysis method, we demonstrated that SCI induced smooth muscle cell (SMC) hypertrophy and changes in orientation of smooth muscle bundles in 10-day SCI bladders.²⁰ Essentially our results to date have demonstrated that the bladder wall exhibits significant tissue remodeling within 10 days following SCI. These results indicate that SCI induces changes in mass composition and microstructure, which in turn, result in alteration of the mechanical properties of bladder wall tissue.

However, SCI is an ongoing pathophysiological process with profound clinical implications. For example, SCI patients continue to suffer from the chronic complications such as noncompliant bladder conditions.¹⁰ Our short-term findings, however, may not represent the longer-term changes following SCI. The objective of the present study was thus to expand the scope of our investigation beyond 10 days after

Address correspondence to Michael S. Sacks, McGowan Institute for Regenerative Medicine, University of Pittsburgh, 100 Technology Drive, Room 234, Pittsburgh, PA 15219, USA. Electronic mail: msacks@pitt.edu

injury, and to evaluate long-term effects of SCI on the bladder wall tissue remodeling and function. To conduct this time-course study, we applied and integrated various experimental methods (including biochemical assays and histomorphometry) to investigate how changes in mechanical properties correlated with alterations in composition and morphology of the bladder wall tissue at various time points up to 10 weeks following the SCI.

METHODS

Specimen Preparation

Female Sprague-Dawley rats (250–300 g) were subjected to complete transection of spinal cord at the T9-T10 level. The animals were treated and cared for according to our protocol approved by Institutional Animal Care and Use Committee (IACUC, University of Pittsburgh, Pittsburgh, PA, USA). The whole urinary bladders were harvested at 1.5-week, 6-week, and 10-week post-SCI and were immediately placed in modified Krebs solution (containing 113 mM NaCl, 4.7 mM KCl, 1.2 mM $\text{MgSO}_4 \cdot 7\text{H}_2\text{O}$, 25 mM NaHCO_3 , 1.2 mM KH_2PO_4 , 5.9 mM Dextrose, and 1 mM EGTA, pH 7.4) and refrigerated at 4 °C for up to 48 h following sacrificing of the animals. Before mechanical testing, the bladders were cut open longitudinally along the urachus and were trimmed down to make square test specimens by removing the dome and trigone sections of the organ (Fig. 1a). Small carbon graphite particles were affixed on the luminal surface of the square bladder specimen for strain measurements and four sides of each specimen were tethered using suture and very small stainless steel hooks. This geometric arrangement produces a central region where the stress and strain fields are relatively homogeneous.²⁵

Biaxial Mechanical Testing

After preparation, each test specimen was mounted on a custom biaxial testing device. Details of biaxial mechanical testing procedures and calculations have been described elsewhere.^{9,22} Briefly, each side of the square test specimen was connected to the motor carriages *via* sutures to apply four-point loads. The load on each axis (circumferential and longitudinal) was constantly monitored using force transducers (with a signal conditioner) and the applied load was controlled by adjusting the stepper motors using our custom software and a data acquisition board installed on a PC. All specimens were tested at room temperature in the modified Krebs solution described. Throughout

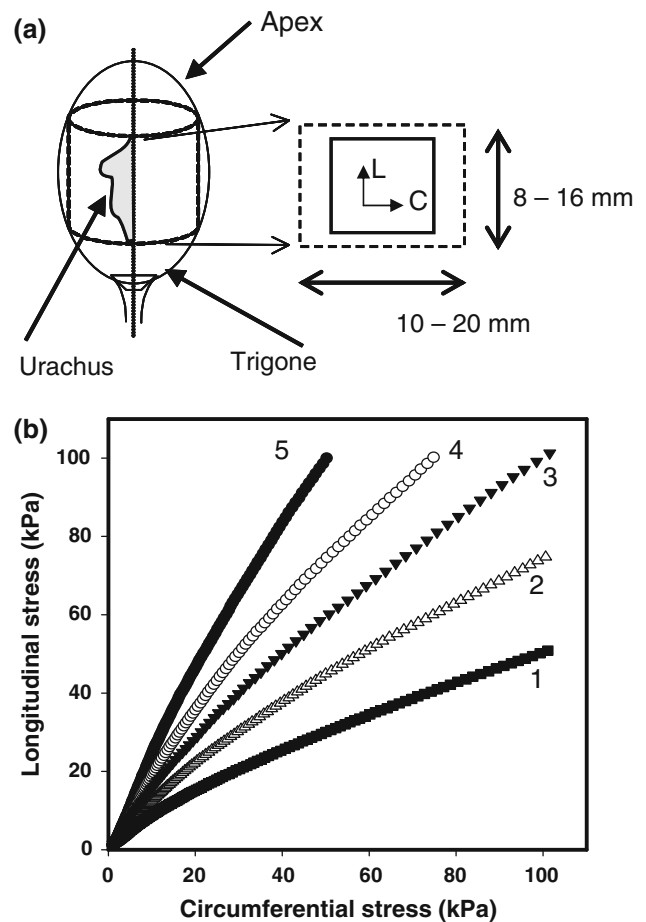


FIGURE 1. (a) Rat bladders were cut open longitudinally along the urachus and a rectangular specimen prepared from tissue. Note that the specimens were oriented with the circumferential (C) and longitudinal (L) directions parallel to the x_1 and x_2 biaxial test axes, respectively. (b) An example of the biaxial testing protocols used for mechanical evaluation of the post-SCI urinary bladder wall (note protocol numbers).

testing, in-plane strain axial stretches were determined from the two-dimensional deformation gradient tensor \mathbf{F} , determined from displacements of four markers affixed to the surface of the specimen using standard methods.²² The resulting Green-Lagrange strain tensor \mathbf{E} was computed using $\mathbf{E} = \frac{1}{2}(\mathbf{F}^T\mathbf{F} - \mathbf{1})$. The data demonstrated the shear components E_{12} were negligible, so that the axial stretches $\lambda_C = F_{11}$ and $\lambda_L = F_{22}$ could be used to describe the total tissue stretch along the test axes.

Biaxial mechanical testing protocols followed those used previously in our laboratory.⁹ Briefly, all tests utilized a constant ratio of the axial Lagrangian normal stresses, $T_{CC}:T_{LL}$, to a peak stress value of 100 kPa. Testing began with an equi-biaxial protocol of $T_{CC}:T_{LL} = 100 \text{ kPa}:100 \text{ kPa}$. After this test, the specimen was returned to the tare-loaded state, and the

marker coordinates used as the reference state for all subsequent strain computations (i.e., the post-pre-conditioned state). Next, five consecutive tests, (Fig. 1b) were performed with $T_{CC}:T_{LL} = 100:50, 100:75, 100:100, 75:100, 50:100$ (in kPa), respectively. These ratios were chosen to cover a wide range of stress states that encompass the known range of physiological responses. A final equi-biaxial test was performed to confirm that the mechanical behavior had not changed during the experiment. Total testing time was approximately an hour and a half for each specimen. Each test consisted of 12 contiguous cycles with a period of 15–25 s to 10–30% strain, resulting in a typical strain rate of $\sim 1\%/s$. Note that in addition to the axial stretches, the areal strain was also computed, which represents the net compliance of the tissue, incorporating stretch effects from both axes. Differences between the maximum axial stretches and areal strains (average \pm SEM) were compared in each group using Mann–Whitney Rank Sum test and the difference was considered significant if $p < 0.05$.

Response Functions

It was assumed that bladder wall could be treated as a pseudo-elastic material based on the tenets originally laid out by Fung.⁷ Central to this approach is that the loading portion of the measured stress–strain response can be treated as a conservative mechanical system, and further treated as a hyperelastic material.^{2,26} Therefore, the in-plane second Piola–Kirchhoff stresses \mathbf{S} can be derived from a scalar strain energy function W through

$$\mathbf{S} = \frac{\partial W}{\partial \mathbf{E}} - p\mathbf{I} \quad (1)$$

where \mathbf{E} is Green–Lagrangian strain tensor, p is a Lagrangian multiplier, and \mathbf{I} is the identity tensor. In the present study, our primary focus was to identify changes in material class (e.g., isotropic, orthotropic, and transverse orthotropic) with the remodeling events in the post-SCI bladder wall under planar biaxial deformations, as a prelude to identification of a strain energy function. Under this special case, p can be removed from Eq. (1) through considering the specific boundary conditions of the planar biaxial loading state.^{11,25}

As in our previous studies,²⁶ we employed a graphical technique to examine the partial derivatives of W with respect to each strain component (or a response function) applied to the wide range of experimental data generated in this study to develop a loading protocol independent of representation of the pseudo-elastic loading behavior. Specifically, biaxial mechanical data

obtained from all test protocols for each stress tensor component were individually fit to the following interpolation functions:

$$\begin{aligned} S_{11} &= \frac{c_{10}}{2} (2c_{11}E_{11} + 2c_{13}E_{22} + 2c_{14}E_{11}E_{22} + c_{15}E_{22}^2 \\ &\quad + 2c_{16}E_{11}E_{22}^2 + 4c_{17}E_{11}^3) \exp P_1 \\ S_{22} &= \frac{c_{20}}{2} (2c_{22}E_{22} + 2c_{23}E_{11} + 2c_{25}E_{22}E_{11} \\ &\quad + c_{24}E_{11}^2 + 2c_{26}E_{11}^2E_{22} + 4c_{28}E_{22}^3) \exp P_2 \end{aligned} \quad (2)$$

where:

$$\begin{aligned} P_1 &= c_{11}E_{11}^2 + c_{12}E_{22}^2 + 2c_{13}E_{11}E_{22} + c_{14}E_{11}^2E_{22} \\ &\quad + c_{15}E_{22}^2E_{11} + c_{16}E_{11}^2E_{22}^2 + c_{17}E_{11}^4 + c_{18}E_{22}^4 \\ P_2 &= c_{21}E_{11}^2 + c_{22}E_{22}^2 + 2c_{23}E_{11}E_{22} + c_{24}E_{11}^2E_{22} \\ &\quad + c_{25}E_{22}^2E_{11} + c_{26}E_{11}^2E_{22}^2 + c_{27}E_{11}^4 + c_{28}E_{22}^4 \end{aligned} \quad (3)$$

and c_{ij} are fitted parameters and E_{ii} (no summation) are the components of Green strain tensor. Note that Eqs. (2) and (3) do not represent a constitutive model, but simply interpolation functions for each axial stress component, and that all shear components were omitted as the data demonstrated very low values of shear. From Eqs. (2) and (3) stress component contours over the experimental strain plane were generated to allow direct examination of material symmetries and to evaluate the material classification.

Assessment of Collagen and Elastin Content of the SCI Rat Bladders

Following biaxial mechanical testing, the 1.5-, 6-, and 10-weeks SCI bladder specimens were cut into 12 strips ($1 \times 10 \text{ mm}^2$ each). These strips were weighed, and six of them were digested in 0.5 N acetic acid supplemented with 1 mg/mL pepsin (Sigma, St. Louis, MO, USA) at 4 °C overnight. Acid-soluble collagen in the supernatant solution was quantified using a commercially available assay kit (Accurate Chemical, Westbury, NY, USA) and following the manufacturer's instructions. In order to digest elastin contents, the remainder six strips were treated with 0.25 M oxalic acid at 95 °C for 180 min (60 min \times 3). Elastin concentrations in these supernatants were also quantified using a commercially available assay kit (Accurate Chemical) and following the manufacturer's instructions. The data, expressed in terms of milligrams per gram of wet tissue weight, were analyzed using unpaired *t*-test when compared to that of normal and 3-week SCI bladders from our previous study,¹⁸ and the *p*-values of <0.05 were considered statistically significant.

Image Analysis of Histological Sections of the SCI Rat Bladders

To elucidate the link between the tissue microstructure and mechanical properties of the wall, we used a novel semi-automated image analysis method to quantify smooth muscle bundle orientation in the bladder wall tissues from 10-week post-SCI rats. To limit the number of animals subjected to the experimental SCI, we performed the histomorphometry study on a select time point. Since the main focus of the study was on the long-term changes, only the data from the longest time point were collected and presented (Figs. 5 and 6). Details of this method have been previously described.²⁰ Briefly, for each bladder specimen, 12 histological sections from the detrusor layer were examined using light microscopy. On average, six fields per section were imaged capturing the entire section without any overlap between the image fields. Digital images of each captured field were obtained and used for detection of the edge of smooth muscle bundles, via custom-made image analysis software. The smooth muscle bundle orientation for each bladder was quantified by first grouping the muscle edge counts (obtained from 72 images per specimen) into 18 angular bins, such that each bin contained the number of edges that lay within an angle span of 10° (i.e., -5°-4°, 5°-14°, 15°-24°, ... 165°-174°). The muscle edge counts in each angular bin were then normalized by the total number of muscle edges for each bladder, and the data were reported as edge count percentages, plotted in the polar coordinate system. To provide a visual clarity, taking advantage of the rotational symmetry of muscle orientation about horizontal axis (e.g., 30° = 210°), the 180°-rotated image of the plot was added to the original graph to construct a 360° polar plot. The mean smooth muscle orientations ($n = 3$) were analyzed by performing the one-way analysis of variance (ANOVA) using a commercial statistics software package (SigmaStat; SPSS Inc., Chicago, IL, USA). This was followed by the Student–Newman–Keuls post hoc test to perform pair-wise comparisons of all the means. The results were compared to that of normal and 10-day SCI bladders from our previous study.²⁰ The p -values of <0.05 were considered statistically significant. Additionally, to quantify the area fraction for tissue components using the image analysis software, the numbers of color-segmented pixels (i.e., red for muscle and yellow for collagen) were counted for all samples. The individual pixel counts for each component were normalized by the total pixel counts of both components (sum of red and yellow pixels, representing the entire tissue section) for each specimen and the data were reported as bladder tissue composition (Fig. 6).

To facilitate comparisons with our previous data, since the results of mechanical testing of SCI bladder specimens were similar to the published results, we included the biomechanical data from Gloeckner *et al.*⁹ for normal and 10-day (1.5-week) SCI groups, and bladder wall tissue composition and morphology from Nagatomi *et al.*²⁰ for normal and 3-week post-SCI. This allowed us to present a reasonably complete picture of short term (normal to 1.5 weeks) and longer term (3–10 weeks) of the biomechanical, morphological, and compositional changes in the urinary bladder wall post-SCI.

RESULTS

Mechanical Properties

Long-term SCI bladder wall tissue, for all biaxial mechanical protocols, demonstrated responses comparable to our previous short-term studies⁹ (Fig. 2). This included the fact that the longitudinal axis demonstrated stretch reversal, but the circumferential direction did not (Fig. 2). Furthermore, there was a significant difference between maximum axial stretches in circumferential and longitudinal directions in all SCI specimens (Fig. 3a). In particular, maximum axial stretch in circumferential direction was significantly ($p < 0.05$) greater than that in longitudinal direction (Fig. 3a) in the normal, 3-, 6-, and 10-week SCI bladders. Overall trends in tissue properties are more clearly revealed when examining the areal stretch (Fig. 3b). Here, SCI bladder specimens in 3, 6, and 10 weeks following injury revealed that the bladder wall tissue compliance was significantly greater ($p < 0.001$) in 3- and 6-week samples compared to that of normal bladders. However, the compliance of 10-week SCI specimens was significantly lower ($p < 0.001$) than 1.5-, 3-, and 6-week SCI samples, and was similar ($p = 0.101$) to the tissue compliance of normal bladders.

Response Functions

From the response functions for each bladder wall two-dimensional contour plots were generated over the realized experimental strain plane to allow direct examination of material symmetries. This allowed evaluation of material class and degree of anisotropy directly from the experimental data (Fig. 4). The existence and direction of marked anisotropy were apparent in normal tissue, with a distinct bias toward the circumferential direction (x_1 -axis). In contrast, 10-day specimens demonstrated a near isotropic response, with a small bias toward the longitudinal

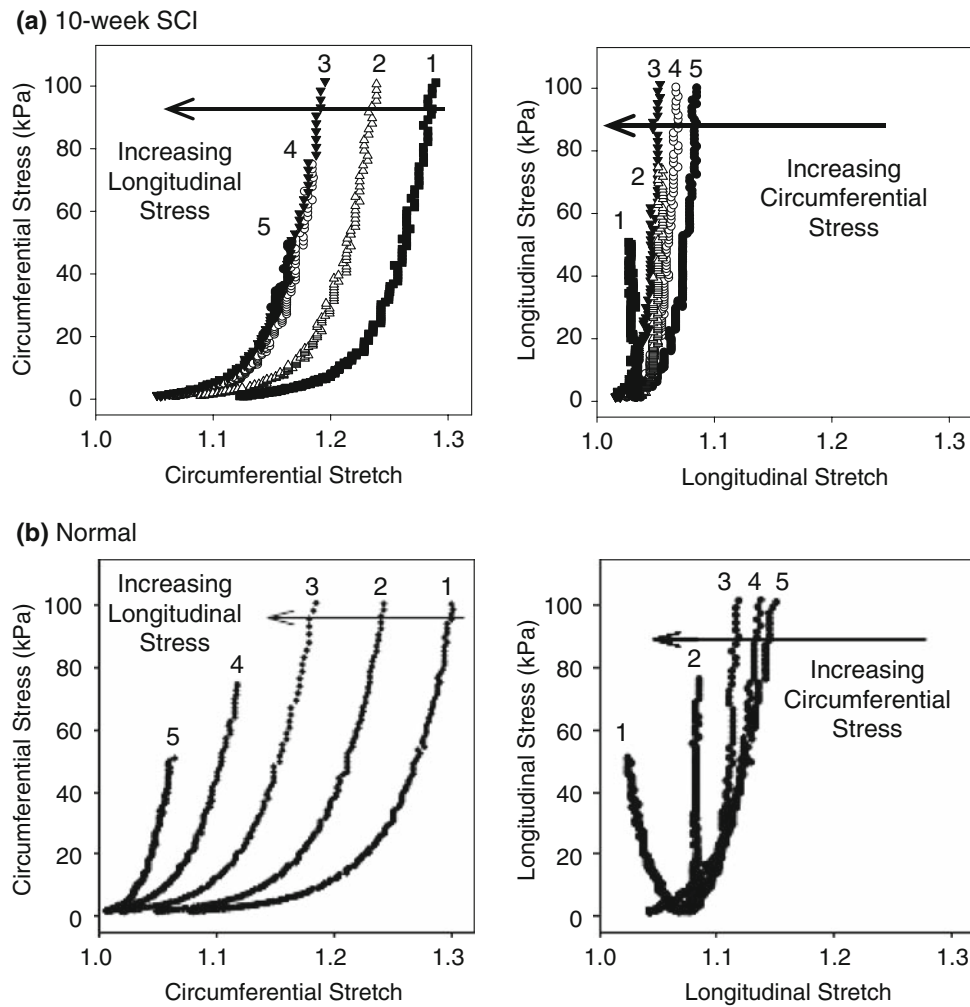


FIGURE 2. Representative stress–strain response to protocols showed in Fig. 1b for a 10-week SCI (*upper panel*), and a normal (*lower panel*, redrawn from Gloeckner⁸ for comparison) urinary bladder wall specimen. Similar to the normal bladder, the 10-week SCI sample demonstrated stretch reversal in the longitudinal axis but not in the circumferential direction.

direction, indicating a reversal of the material axes. Interestingly, this trend was reversed at 10-weeks SCI, where there was marked strong alignment to the x_1 (i.e., circumferential) stretch axis. Further, at this time point the distance between the contours at large strains was narrowed near the E_{11} axis compared to the E_{22} axis, indicating a strong dependence of W on E_{11} . These results indicate that the profound changes in tissue compliance (Fig. 3) were accompanied by substantial changes in material class.

Muscle Fiber Orientation and Its Relation to Tissue Mechanical Response

Fiber orientation results overall followed the trends observed in biomechanical responses (Fig. 5). Results from the 10-week SCI specimens demonstrated that orientation of smooth muscle fibers was sharply aligned to the longitudinal axis of bladder. Specifically,

the normalized muscle edge counts in 75° – 84° , 85° – 94° , 95° – 104° and 105° – 114° angle spans (with the mean ranging from $11.45 \pm 2.48\%$ to $17.88 \pm 3.34\%$) were significantly greater ($p < 0.05$) compared to those in all the other directions whose average values were $< 5\%$ (Fig. 5c, upper panel). The observed changes in fiber orientation clearly paralleled the observed changes in mechanical responses (Figs. 4 and 5, lower panels). These findings suggest that both the changes in material class and axial peak strains were a result of the alterations in bladder wall tissue architecture, namely the extracellular matrix (ECM) composition and SMC orientations.

Compositional Changes in the Rat Bladder Following Long-term SCI

The wet weights of SCI bladder specimens at all time points were significantly higher than those of

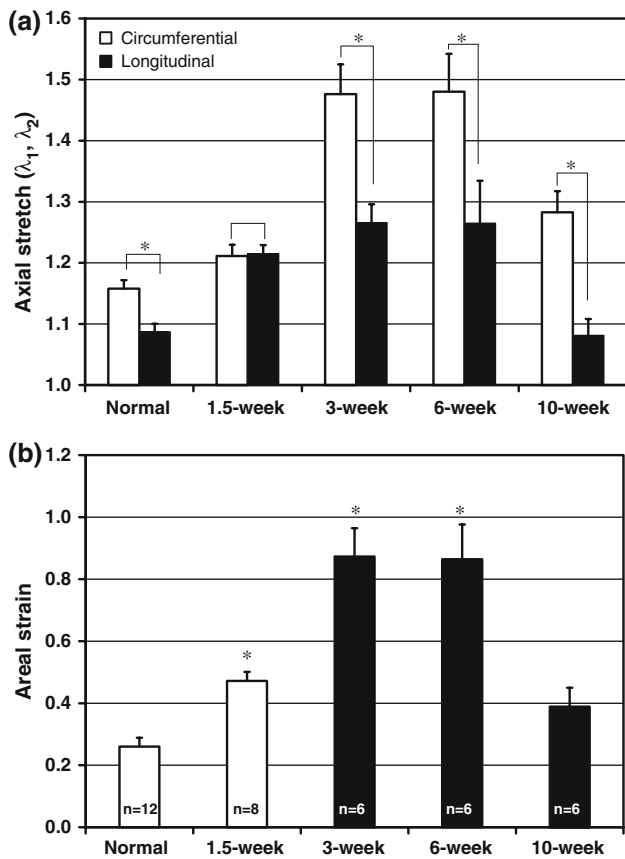


FIGURE 3. (a) Maximum axial stretches in circumferential and longitudinal directions in normal and 1.5-, 3-, 6-, and 10-week SCI rat bladders. Data are shown as mean \pm SEM where * indicates $p < 0.05$ between two directions. (b) Corresponding maximum areal strain (white bars were redrawn from Gloeckner *et al.*⁹). Data are shown as mean \pm SEM where * indicates $p < 0.05$ from normal and 10-week SCI tissue.

normal bladders, with the 10-week specimens nearly double the normal value (Table 1). Elastin mass and concentration values at 1.5-, 3-, 6-, and 10-week SCI bladders all increased dramatically compared to normal values (Table 1). The total collagen mass declined overall up to 6 weeks post-SCI, while collagen concentrations (collagen mass normalized by bladder sample wet weight) of the normal bladders and 1.5-, 3-, and 6-weeks SCI bladders were similar to each other (Table 1). The collagen mass rose considerably at 10 weeks, and as a result, collagen concentration of 10-week SCI specimens was significantly ($p < 0.05$) greater than other SCI groups, but similar to that of normal. Additionally, semi-automated image analyses of histological sections of rat bladder tissues revealed that the collagen area fractions in the 10-week SCI bladders were significantly ($p < 0.05$) higher compared to the 10-day SCI group, but were similar to the normal bladders (Fig. 6).

Relation Between Compositional and Mechanical Property Changes

While the relation between tissue composition and mechanical response is intuitive, the results of the present study allow for additional insights. Specifically, the ratio of elastin/collagen mass has been suggested as an index in determining the compliance of the obstructed bladder.¹³ We computed this index from the data presented in Table 1 and compared it to the areal strain for each time point (Fig. 7). Qualitatively, an overall strong correlation was observed, suggesting a causal relation between this ratio and the time-course changes in bladder wall tissue mechanical properties after SCI.

DISCUSSION

Changes in the Mechanical Properties of Bladder Wall

Previously, we demonstrated that the urinary bladder wall compliance in 10-day SCI rats was significantly greater when compared to the normal bladders.⁹ The present study builds on these findings by demonstrating changes in bladder wall tissue for up to 10 weeks following injury. While overall tissue compliance continued to increase for up to 6 weeks, a drastic decrease was observed at 10 weeks (Fig. 3). Based on clinical reports of hypocompliance from chronic SCI patients, we speculate that bladder wall compliance may decrease even further for a period longer than 10-week post-injury.¹⁰

Changes in the biomechanical response of the bladder wall tissue extended beyond changes in overall compliance. Specifically, changes in material class from anisotropic (in normal rats) to isotropic (in 1.5-week SCI rats) to anisotropic (in 10-week SCI rats), indicated continual remodeling after SCI. These changes were in agreement with alterations in composition and structure of the 10-week SCI bladders, and supported the close correlation between changes in structure/composition and mechanical properties of the bladder tissue. This finding further indicates that changes in bladder wall properties are thus not only the relative quantities of the individual tissue phases (smooth muscle, collagen, and elastin), but also a result of changes in architecture.

Bladder Wall Model Material Class and Changes in Architecture

One focus of the present study was to provide insight into the mechanical characteristics of the urinary bladder wall as a prelude to development of constitutive models for the remodeling bladder wall

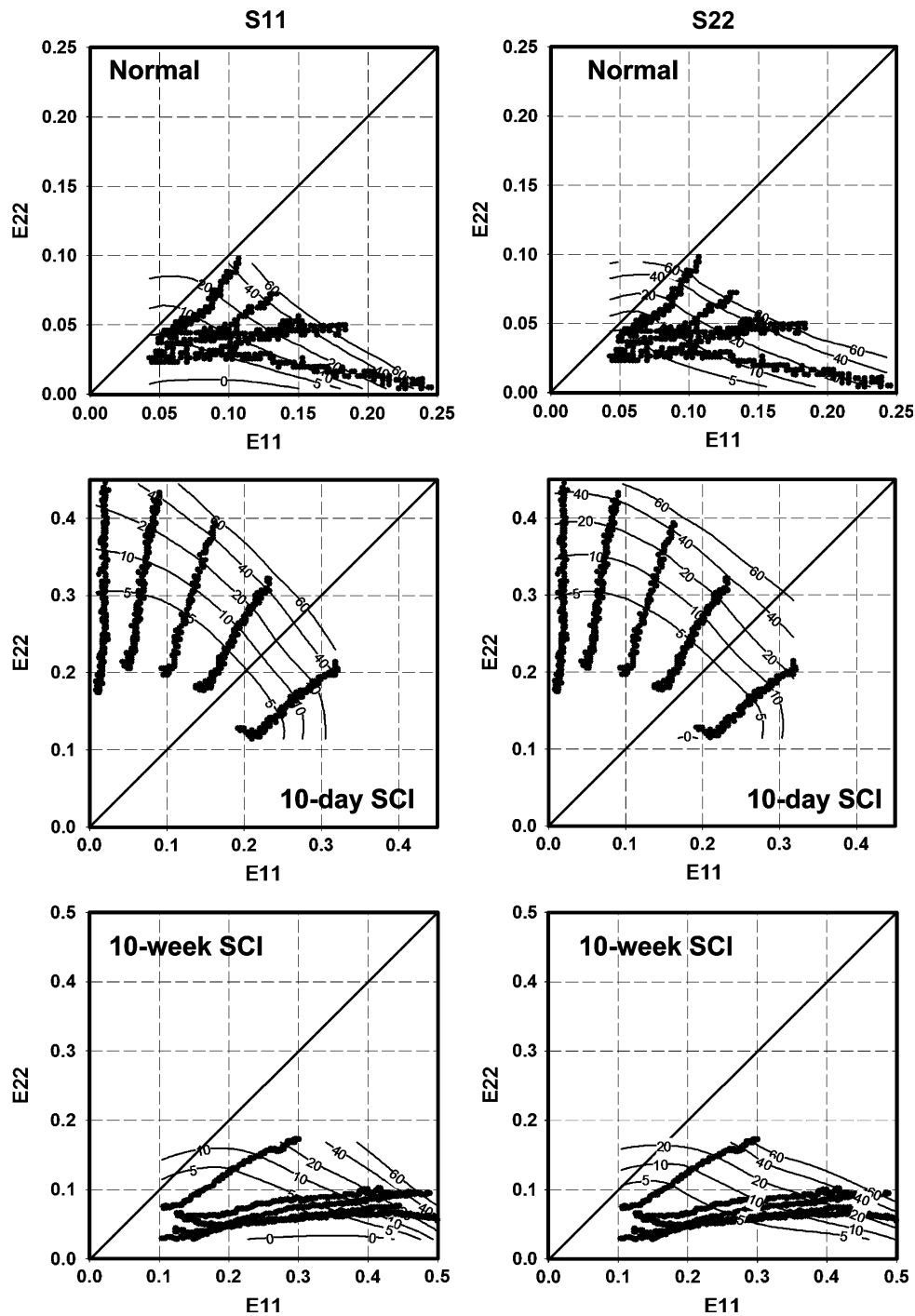


FIGURE 4. Representative response function (S_{11} and S_{22}) contours for normal, 10-day SCI (data taken from Gloeckner⁸), and 10-week SCI rat bladder wall drawn over the experimentally measured strain plane. Solid diagonal lines are the $E_{11} = E_{22}$ identity, shown for visual reference, along with contour lines whose relative densities indicate local stiffness gradients. Marked changes in anisotropic behavior were observed from normal for all time points, indicating presence of time dependent tissue remodeling.

tissue. Thus, it is first desirable to evaluate the multi-axial mechanical behavior of the time-course changes independent of any specific constitutive model form. In the present study, a straightforward graphical approach previously developed for our studies of

cardiovascular tissues,^{26,28} was used to characterize the strain-energy function to determine changes in the material class. The response functions provided a useful approach visualizing the stress response over the entire measured strain region. We observed in normal

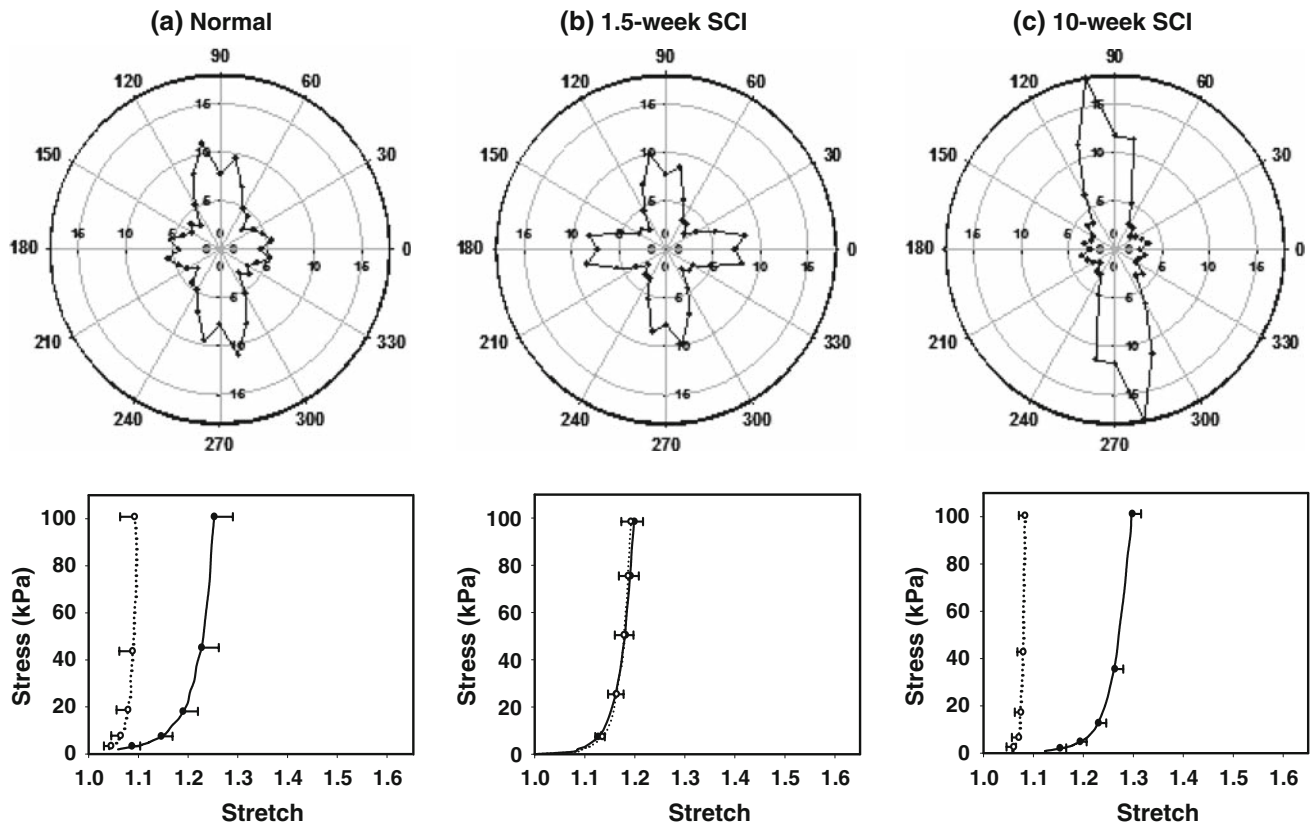


FIGURE 5. Upper panel: orientation distribution of smooth muscle bundles in normal (a), 1.5-week SCI (redrawn from Nagatomi *et al.*²⁰) (b) and 10-week SCI (c) bladders. Lower panel: The longitudinal (○) and circumferential (●) stress-stretch curves representing actual data points collected during equi-biaxial stress protocol (mean \pm SEM). At all time points the changes in preferred muscle orientation corroborated the mechanical anisotropy data.

TABLE 1. Specimen wet weights, collagen, and elastin mass and concentration (mass/wet weight) in the normal and SCI rat bladders.

Time (weeks)	Sample size (n)	Wet weight (g)	Collagen mass (mg)	Collagen conc. (mg/g)	Elastin mass (mg)	Elastin conc. (mg/g)
Normal	7–10	0.099 \pm 0.010	1.56 \pm 0.179	16.9 \pm 2.81	0.029 \pm 0.017	0.321 \pm 0.056
1.5	5	0.127 \pm 0.006*	1.32 \pm 0.098	10.5 \pm 1.04	0.105 \pm 0.031*	0.886 \pm 0.083*
3	6–7	0.162 \pm 0.019*	1.48 \pm 0.157	9.63 \pm 1.00	0.152 \pm 0.078*	1.18 \pm 0.131*
6	5	0.130 \pm 0.016*	1.09 \pm 0.063	8.40 \pm 0.851	0.138 \pm 0.024*	1.23 \pm 0.286*
10	4	0.211 \pm 0.017*	2.54 \pm 0.157**	12.2 \pm 0.791***	0.218 \pm 0.026*	1.06 \pm 0.101*

Data are presented as mean \pm SEM, with * indicating different from normal, ** indicating different from all groups, and *** indicating different from all SCI groups but similar to normal, analyzed by one-way ANOVA followed by the Student–Newman–Keuls post hoc test. Data for Normal and 3 weeks were taken from Nagatomi *et al.*¹⁸

tissues substantial anisotropy, with a strong bias toward the circumferential direction (Fig. 4) and substantially higher stress gradients at higher strain levels. In contrast, the 10-day SCI group exhibited a slight symmetrical response about equi-strain line, a more compliant response along the longitudinal direction, and overall much lower stress level gradients at higher strain levels. Interestingly, the 10-week SCI group demonstrated a response much closer to normal tissue complete asymmetry with more dependence of W on E_{11} when compared to the normal and 10-day SCI bladders.

Perhaps the most interesting finding of the present study is that the mechanical response of all three groups correlated very closely to the measured changes in smooth muscle orientation (Fig. 5). Nagatomi *et al.*²⁰ have observed that the early changes in mechanical properties (i.e., up to 10 days) are a direct result of rapid, pronounced bladder wall tissue remodeling, including changes in the bladder wall tissue architecture, such as SMC orientation. Reviewing the previous results also reveals that dominant distribution of muscle bundles in longitudinal direction in normal bladders was mirrored by mechanical anisotropy in those

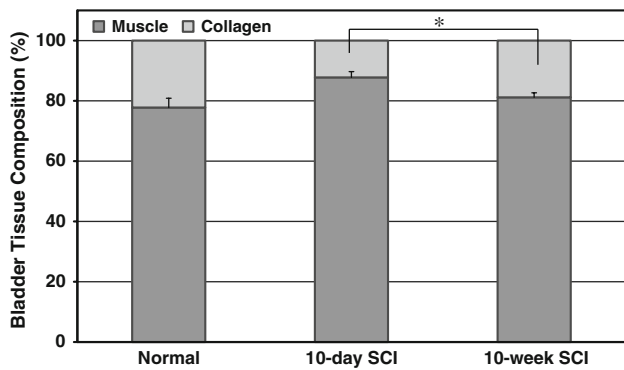


FIGURE 6. Area fractions of muscle and collagen in normal, 10-day (redrawn from Nagatomi *et al.*²⁰) and 10-week SCI rat bladders, fixed at 50% volume capacity. The 10-week SCI bladders exhibited significant increases in collagen area fractions compared to the 10-day SCI group, but similar to the normal bladders. Data are mean \pm SD; $n = 3-5$; analyzed by one-way ANOVA followed by the Student–Newman–Keuls post hoc test; with * indicating $p < 0.05$.

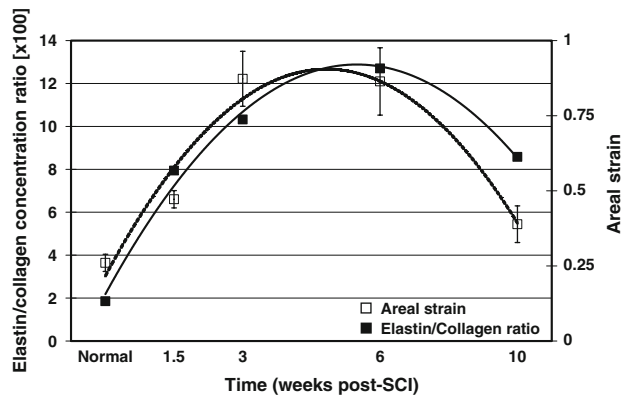


FIGURE 7. Peak areal strain (a measure of total tissue compliance) and elastin/collagen mass ratio vs. time. While the initial increases in the elastin/collagen ratio result from upregulation of elastin production, the decrease after 6 weeks is due to substantial upregulation of collagen production, which occurred even in the presence of continued elastin production at 10 weeks.

specimens, and bimodal orientation observed in 10-day SCI bladders resulted in an isotropic behavior of bladder wall tissue (Fig. 4). The results of the present study provided extended evidence that changes in the orientation of smooth muscle bundles significantly contribute to the alteration in material class of bladder tissue (Fig. 5). Taken as a whole, these findings indicate a profound, complex biomechanical remodeling process in the urinary bladder wall post-SCI.

Changes in the Rat Bladder Composition Following Long-Term SCI

It has been postulated that the mechanical properties of the bladder wall are largely determined by those of

the ECM components.^{1,13,14,16} In particular, collagen and elastin are two major connective tissue proteins providing urinary bladder tissue, with tensile strength and elasticity, respectively. Alterations in content or intrinsic properties of either of these proteins may lead to changes in bladder functional properties.^{16,23}

The results of present study provided evidence that the SCI groups at all time points examined had higher elastin contents compared to the normal bladders (Table 1). This finding indicated an early response to changes in mechanical environment (e.g., over-distension due to lack of micturition reflex)^{4,18,31} that contributed to an increased compliance in 10-day SCI samples compared to the normal bladders.

The collagen concentration, on the other hand, appeared to decline up to 6 weeks after injury, due to increased bladder mass, secondary to smooth muscle hypertrophy. The collagen content eventually rose at 10 weeks, and as a result, collagen concentration of 10-week SCI specimens was considerably greater than all other SCI groups, and became similar to that of normal (Table 1). The higher collagen concentration of 10-week SCI bladders was consistent with increased collagen area fractions in this group (Fig. 6), and indicated that collagen production significantly amplified by 10 weeks post-injury; therefore, collagen increase in mass fraction superseded that of smooth muscle. These findings suggest that increased collagen content is a late response to altered mechanical environment of bladder wall, which presumably happened between 6 and 10 weeks post-injury.

Moreover, the close and parallel changes of the elastin/collagen ratio and bladder compliance (Fig. 7) suggest that the alterations in bladder wall mechanical properties are in large part induced by pronounced synthesis and deposition of ECM components. While elastin content of SCI samples at all time points remained higher than that of normal bladder, collagen content increased significantly at 10 weeks after SCI. Taken as a whole, these results suggest that collagen production increases dramatically after 6 weeks, and by 10 weeks dominates over the effects of elastin production resulting in markedly stiffened bladder wall.

While the current results are the first to exhibit such changes in SCI rat bladders, they are also consistent with the patterns observed in mechanically obstructed bladders, including tissue hypertrophy, and increased elastin contents.^{13,27} Kim *et al.*¹² have observed rapid hypertrophy characterized by increased bladder mass and collagen deposition in bladder outlet obstruction. The total amount of collagen increased after obstruction and decreased after relief; however, collagen concentration decreased after obstruction and increased following relief. The protein deposition of types I and III collagen was localized in lamina propria

and muscle bundles in all groups. The expression of types I and III collagen gene was up regulated after obstruction, but down regulated after relief. Also, significant negative correlation between contractility and gene expressions of collagen types was observed. These data suggest that the change in localization and quantity of collagen types leads to morphologic changes of bladder and can have an impact on the contractility. Clearly, further biochemical analysis of the rat bladder wall, especially quantification of crosslinking for ECM proteins and/or collagen typing, will be required to validate the link between alterations of the bladder compliance and changes in its composition following SCI.

CONCLUSIONS

The results of present study suggest that changes in bladder composition and smooth muscle fiber structure are responsible for the alteration in mechanical behavior of bladder after SCI. Bladder wall compliance was found to be significantly greater at 3- and 6-weeks when compared to the normal bladders, but at 10-weeks compliance substantially reduced to near that of normal bladders. This trend in mechanical compliance closely paralleled the collagen/elastin ratio. While the initial increases in the elastin/collagen ratio result from upregulation of elastin production, the decrease after 6 weeks is due to substantial upregulation of collagen production after 6 weeks, which occurred even in the presence of continued elastin production at 10 weeks. Moreover, changes in material class correlated closely with quantitative changes in smooth muscle fiber orientation. The results of the present study provide the first evidence that acute and chronic responses of the urinary bladder wall tissue to SCI are distinct, result in profound and complex time dependent changes in bladder wall structure, and will lay the basis for simulations of the bladder wall disease process.

ACKNOWLEDGMENTS

The authors wish to acknowledge funding by NICDH P01-HD39768 and the Paralyzed Veterans of America Spinal Cord Research Foundation (#2289-01). KKT was supported by an NIH T32 training grant (DK7774). The authors wish to also thank Drs. Kazumasa Torimoto and Teruyuki Ogawa for providing the rat bladders used in this study, and Ms. Silvia Wognum for technical assistance.

REFERENCES

- ¹Cortivo, R., F. Pagano, G. Passerini, G. Abatangelo, and I. Castellani. Elastin and collagen in the normal and obstructed urinary bladder. *Br. J. Urol.* 53(2):134–137, 1981.
- ²Criscione, J. C., M. S. Sacks, and W. C. Hunter. Experimentally tractable, pseudo-elastic constitutive law for biomembranes: I. Theory. *J. Biomech. Eng.* 125(1):94–99, 2003. doi:10.1115/1.1530770.
- ³de Groat, W. C. A neurologic basis for the overactive bladder. *Urology* 50(6A Suppl):36–52, 1997; discussion 53–56.
- ⁴de Groat, W. C., A. M. Booth, and N. Yoshimura. Neurophysiology of micturition and its modification in animal models of human disease. In: *Nervous Control of the Urogenital System*, Vol. 3, edited by C. A. Maggi. Chur: Harwood Academic Publishers, 1993, pp. 227–290.
- ⁵Deveaud, C. M., E. J. Macarak, U. Kucich, D. H. Ewalt, W. R. Abrams, and P. S. Howard. Molecular analysis of collagens in bladder fibrosis. *J. Urol.* 160(4):1518–1527, 1998. doi:10.1016/S0022-5347(01)62606-5.
- ⁶Drake, M. J., P. Hedlund, I. W. Mills, R. McCoy, G. McMurray, B. P. Gardner, K. E. Andersson, and A. F. Brading. Structural and functional denervation of human detrusor after spinal cord injury. *Lab. Invest.* 80(10):1491–1499, 2000.
- ⁷Fung, Y. C. *Biomechanics: Mechanical Properties of Living Tissues*. New York: Springer Verlag, 1993.
- ⁸Gloeckner, D. C. *Tissue Biomechanics of the Urinary Bladder Wall*. Pittsburgh: Department of Bioengineering, University of Pittsburgh, 258 p, 2003.
- ⁹Gloeckner, D. C., M. S. Sacks, M. O. Fraser, G. T. Somogyi, W. C. de Groat, and M. B. Chancellor. Passive biaxial mechanical properties of the rat bladder wall after spinal cord injury. *J. Urol.* 167(5):2247–2252, 2002. doi:10.1016/S0022-5347(05)65137-3.
- ¹⁰Hackler, R. H., M. K. Hall, and T. A. Zampieri. Bladder hypocompliance in the spinal cord injury population. *J. Urol.* 141(6):1390–1393, 1989.
- ¹¹Humphrey, J. D. *Cardiovascular Solid Mechanics: Cells, Tissues, and Organs*. New York: Springer, 2002.
- ¹²Kim, J. C., J. Y. Yoon, S. I. Seo, T. K. Hwang, and Y. H. Park. Effects of partial bladder outlet obstruction and its relief on types I and III collagen and detrusor contractility in the rat. *Neurourol. Urodyn.* 19(1):29–42, 2000. doi:10.1002/(SICI)1520-6777(2000)19:1<29::AID-NAU5>3.0.CO;2-#.
- ¹³Kim, K. M., B. A. Kogan, C. A. Massad, and Y. C. Huang. Collagen and elastin in the obstructed fetal bladder. *J. Urol.* 146(2 (Pt 2)):528–531, 1991.
- ¹⁴Kondo, A., and J. G. Susset. Viscoelastic properties of bladder. *Investigat. Urol.* 11(6):459–465, 1974.
- ¹⁵Kruse, M. N., L. A. Bray, and W. C. de Groat. Influence of spinal cord injury on the morphology of bladder afferent and efferent neurons. *J. Auton. Nerv. Syst.* 54(3):215–224, 1995. doi:10.1016/0165-1838(95)00011-L.
- ¹⁶Macarak, E. J., D. Ewalt, L. Baskin, D. Coplen, H. Koo, R. Levin, J. W. Duckett, H. Snyder, J. Rosenbloom, and P. S. Howard. The collagens and their urologic implications. *Adv. Exp. Med. Biol.* 385:173–177, 1995.
- ¹⁷Mimata, H., F. Satoh, T. Tanigawa, Y. Nomura, and J. Ogata. Changes of rat urinary bladder during acute phase of spinal cord injury. *Urol. Int.* 51(2):89–93, 1993.
- ¹⁸Nagatomi, J., D. C. Gloeckner, M. B. Chancellor, W. C. DeGroat, and M. S. Sacks. Changes in the biaxial

- viscoelastic response of the urinary bladder following spinal cord injury. *Ann. Biomed. Eng.* 32(10):1409–1419, 2004. doi:[10.1114/B:ABME.0000042228.89106.48](https://doi.org/10.1114/B:ABME.0000042228.89106.48).
- ¹⁹Nagatomi, J., K. Toosi, M. Chancellor, and M. Sacks. Contribution of the extracellular matrix to the viscoelastic behavior: A new modeling approach for rat bladder wall tissue. *Biomech. Model. Mechanobiol.*, 2007. [Epub ahead of print].
- ²⁰Nagatomi, J., K. K. Toosi, J. S. Grashow, M. B. Chancellor, and M. S. Sacks. Quantification of bladder smooth muscle orientation in normal and spinal cord injured rats. *Ann. Biomed. Eng.* 33(8):1078–1089, 2005. doi:[10.1007/s10439-005-5776-x](https://doi.org/10.1007/s10439-005-5776-x).
- ²¹Ogawa, T. Bladder deformities in patients with neurogenic bladder dysfunction. *Urol. Int.* 47(Suppl 1):59–62, 1991.
- ²²Sacks, M. S. Biaxial mechanical evaluation of planar biological materials. *J. Elast.* 61:199–246, 2000. doi:[10.1023/A:1010917028671](https://doi.org/10.1023/A:1010917028671).
- ²³Sandberg, L. B., N. T. Soskel, and J. G. Leslie. Elastin structure, biosynthesis, and relation to disease states. *N Engl J. Med.* 304(10):566–579, 1981.
- ²⁴Shin, J. C., C. I. Park, H. J. Kim, and I. Y. Lee. Significance of low compliance bladder in cauda equina injury. *Spinal Cord* 40(12):650–655, 2002. doi:[10.1038/sj.sc.3101380](https://doi.org/10.1038/sj.sc.3101380).
- ²⁵Sun, W., M. S. Sacks, and M. J. Scott. Effects of boundary conditions on the estimation of the planar biaxial mechanical properties of soft tissues. *J. Biomech. Eng.* 127(4):709–715, 2005. doi:[10.1115/1.1933931](https://doi.org/10.1115/1.1933931).
- ²⁶Sun, W., M. S. Sacks, T. L. Sellaro, W. S. Slaughter, and M. J. Scott. Biaxial mechanical response of bioprosthetic heart valve biomaterials to high in-plane shear. *J. Biomech. Eng.* 125:372–380, 2003. doi:[10.1115/1.1572518](https://doi.org/10.1115/1.1572518).
- ²⁷Uvelius, B., and A. Mattiasson. Collagen content in the rat urinary bladder subjected to infravesical outflow obstruction. *J. Urol.* 132(3):587–590, 1984.
- ²⁸Vande Geest, J. P., M. S. Sacks, and D. A. Vorp. The effects of aneurysm on the biaxial mechanical behavior of human abdominal aorta. *J. Biomech.* 39(7):1324–1334, 2006. doi:[10.1016/j.jbiomech.2005.03.003](https://doi.org/10.1016/j.jbiomech.2005.03.003).
- ²⁹Watanabe, T., D. A. Rivas, and M. B. Chancellor. Urodynamics of spinal cord injury. *Urol. Clin. North Am.* 23(3):459–473, 1996. doi:[10.1016/S0094-0143\(05\)70325-6](https://doi.org/10.1016/S0094-0143(05)70325-6).
- ³⁰Weld, K. J., M. J. Graney, and R. R. Dmochowski. Differences in bladder compliance with time and associations of bladder management with compliance in spinal cord injured patients. *J. Urol.* 163(4):1228–1233, 2000. doi:[10.1016/S0022-5347\(05\)67730-0](https://doi.org/10.1016/S0022-5347(05)67730-0).
- ³¹Yoshimura, N., C. P. Smith, M. B. Chancellor, and W. C. de Groat. Pharmacologic and potential biologic interventions to restore bladder function after spinal cord injury. *Curr. Opin. Neurol.* 13(6):677–681, 2000. doi:[10.1097/00019052-200012000-00011](https://doi.org/10.1097/00019052-200012000-00011).